Materials Science and Engineering B 211 (2016) 94–100

Contents lists available at ScienceDirect

Materials Science and Engineering B

journal homepage: www.elsevier.com/locate/mseb

Relative recoilless F-factors in $REFeO_3$ (RE = rare-earth La, Pr, Nd and Sm) orthoferrites synthesized by self-combustion method

L.A Morales [a], G. Sierra-Gallego [a], C.A. Barrero [b], O. Arnache [b,*]

[a] Departamento de Materiales y Minerales, Facultad de Minas, Universidad Nacional de Colombia, Calle 75 # 79A-51, Bloque M17, Medellín, Colombia
[b] Grupo de Estado Sólido, Instituto de Física, Universidad de Antioquia, Calle 70 No. 52-21, A.A. 1226, Medellín, Colombia

ARTICLE INFO

Article history:
Received 4 February 2016
Received in revised form 30 May 2016
Accepted 7 June 2016
Available online 13 June 2016

Keywords:
Orthoferrite
Relative F-factor
Self-combustion

ABSTRACT

In this work, rare-earth orthoferrites polycrystalline compounds $REFeO_3$ (REFO) with RE = rare-earth La, Pr, Nd and Sm were synthesized by the self-combustion method. A direct correlation between the magnitude of the magnetic hyperfine field and the Fe—O_1—Fe bond angles was observed. From transmission Mössbauer spectra recorded at room-temperature, relative recoilless F-factors for these REFO compounds were estimated. The method applied to perform this calculation was based on the determination of two subspectral areas present in a mixture of known amounts of the compound under study and a standard sample (α-Fe). For that purpose spectra were thickness-corrected and fitted using lorentzian lines. The so obtained factors were $F\text{-}_{REFeO3}$ (RE = rare-earth La, Pr, Nd and Sm): 1.30 ± 0.02, 1.08 ± 0.04, 1.15 ± 0.05, 1.18 ± 0.08 respectively. The absolute recoilless factors obtained by this method had an average relative error around 11% in comparison with the values predicted by the Debye model.

1. Introduction

The rare-earth orthoferrites $REFeO_3$ (REFO) are a family of oxides with distorted perovskite structure which show unusual and interesting magnetic properties [1,2]. These materials are canted antiferromagnets and have attracted much attention; first, for their special antisymmetric exchange interaction, which results in weak ferromagnetism [3], and second, for their potential use in spintronic applications (spin valves, sensors) [4,5], as they show spin reorientation phenomena induced by temperature or by an applied magnetic field [6–9]. Moreover, it is worth noting that one of the main components of the orthoferritas are the rare earths elements (REE) such as La, Pr, Nd, and Sm. Nowadays the REE, due to their unique electronic structure and the unique properties of the 4f electron orbitals, are very important elements for industry and have several applications in multiple fields. However, the world is passing by a crisis related with the demand and supply of REE due to their scarceness and how are distributed the REE deposits. Because of the absence of primary deposits to exploit on their territory, many countries will have to draw on recycling of REE from industrial residues and REE-containing end-of-life products. Nevertheless in spite of their importance in the electronic devices REE constitute a small fraction of weight/volume of a final product. In consequence, the exploit percentage is about the same as the poorer ore bodies (i.e., ∼2%) from where REE are mined. In this sense a good tool to detect, identify and quantify rare-earth orthoferrites in samples of complex composition is quite desirable and useful [10,11]. Taking into account the above and considering the interesting magnetic properties of REFO compounds, most of the Mössbauer spectroscopy studies on orthoferrites have been focused on the comprehension of their weak ferromagnetism and the temperature dependence of the sublattice magnetization [12]. These compounds are magnetically ordered over a wide range of temperatures and therefore their Mössbauer parameters differ between the individual species. Thus, the technique is frequently used for the unequivocal distinction and detection of minor amounts of iron oxides, and often for its quantification in systems of complex compositions, taking advantage of the insensitivity of Mössbauer spectroscopy to all isotopes, except those under interest [13]. However, for quantitative Mössbauer characterization of a sample in which two or more iron compounds are present, it is necessary to take into account the recoil-free fraction (f) of each phase. This parameter is defined as the probability of a nucleus in a specific environment at a given temperature to present absorption and emission of gamma rays without recoil [14].

The recoilless f-factor can be calculated by using three methods: (1) the temperature dependence of the absolute subspectral area (A), (2) the temperature dependence of the isomer shift (δ), and (3) the ratio of subspectral areas of two different materials at a given temperature, one of these used as a reference. Methods (1) and (2) usually use the Debye model. For example, Eibschütz

* Corresponding author.
E-mail address: oscar.arnache@udea.edu.co (O. Arnache).

http://dx.doi.org/10.1016/j.mseb.2016.06.005
0921-5107/

et al. [7] collected the Mössbauer spectra of the orthoferrites at different temperatures and studied the temperature dependence of the hyperfine parameters, and by using the Debye method, they derived the Debye temperature (θ_D). On the contrary, method (3) does not depend of the lattice vibration model, and the relative recoilless F-factors is obtained. This last method has been proven to be comparatively much simpler [13–19]. In our work, we use method (3). In this sense, the aim of this work was to find the room-temperature relative recoilless F-factors of four oxide compounds of the rare-earth orthoferrite family REFO (RE = rare-earth La, Pr, Nd and Sm) relative to α-iron which is commonly used as reference for these calculations. Compounds were synthesized by a self-combustion method and then characterized by X-ray diffraction (XRD), scanning electron microscopy (SEM) and energy X-ray dispersive spectroscopy (EDX) measurements. Then, a discussion was made on the possible relation between their structural nature and the values of F-factors. Finally, with the idea of evaluating the effectiveness of this method, the *f* fractions derived from this calculation were compared to those calculated using the Debye temperatures previously reported in literature for these compounds [12].

2. Theory

Using the Debye approximation the probability of recoil-free emission or absorption events (*f*) can be described by the following equation [13,16]:

$$f = exp - \left\{ \frac{3E_\gamma^2}{k_B M \theta_D c^2} \left[\frac{1}{4} + \left(\frac{T}{\theta_D} \right)^2 \int_0^{\theta_D/T} \frac{x dx}{e^x - 1} \right] \right\} \quad (1)$$

where E_γ, k_B, M, θ_D, c, and T are the gamma ray energy, the Boltzmann's constant, the mass of the iron ^{57}Fe nucleus, Debye temperature, the speed of light, and the temperature, respectively.

As can be seen in Eq. (1), *f* is closely related to the strength of the atomic bonding and the vibrations in the solid, in which the Mössbauer nucleus is embedded [17] and it is clear that as the Debye temperature of the crystal becomes higher, *f* becomes higher as well [18]. This means that at a given temperature, the probability of a compound to show recoil-free emission or absorption events increases with the strength of bonds [19].

As has already been mentioned, the use of the Debye approximation to calculate *f* is complicated because it implies collecting several spectra under different temperatures, adjusting the temperature dependence of the isomer shift (δ) or of the subspectral area (A) to calculate the Debye temperature and finally, replacing it in Eq. (1). In comparison, determining the relative recoilless fraction (F) implies an easier procedure, since F is defined as the ratio of the recoil free fractions of two different materials. When the thin absorber condition is satisfied, the subspectral areas (*A*) are proportional to the product of the number of ^{57}Fe atoms (*N*) and the recoil-free fraction (*f*) of each compound [15].

$$\frac{A_a}{A_r} = \frac{f_a N_a}{f_r N_r} \quad (2)$$

$$F_a = \frac{f_a}{f_r} = \frac{A_a N_r}{A_r N_a} \quad (3)$$

where F_a is the relative recoilless fraction of the compound *a* with respect to a reference compound *r* and f_i, A_i, N_i are the recoil free fraction, the Mössbauer sub-spectral area and the total number of ^{57}Fe atoms in the ith-compound, respectively. N_i can be estimated as follows [15]:

$$N_i = \frac{a m_i O_i N_0 N_{i,m}}{MW_i} \quad (4)$$

where a, m_i, O_i, N_0, $N_{i,m}$ and MW_i are the natural abundance of ^{57}Fe ($a = 0.0217$), the mass of the compound, the occupancy fraction, the Avogadro's constant ($N_0 = 6.022 \times 10^{23}$ mol^{-1}), the number of iron atoms per unit formula and the molecular weight, respectively. In this case, the final expression for the F-factor of the $REFeO_3$ orthoferrites (F_{REFO}) relative to alpha-iron (α-Fe) as a function of their sub-spectral areas was obtained by replacing Eq. (4) in (3), thus:

$$F_{REFO} = \frac{m_{\propto Fe} A_{REFO}}{m_{REFO} A_{\propto FE}} C_{REFO} \quad (5)$$

$$C_{REFO} = \frac{O_{\propto Fe} N_{\propto FE,m} MW_{REFO}}{O_{REFO} N_{REFO,m} MW_{\propto Fe}} \quad (6)$$

where $m_{\propto Fe}$, $O_{\propto Fe}$, $N_{\propto Fe}$, and $MW_{\propto Fe}$ are the mass, the occupation fraction, the number of Fe atoms per unitary formula and the molecular weight of alpha-iron, respectively. On the other hand, m_{REFO}, O_{REFO}, N_{REFO} and MW_{REFO} are the mass, occupation fraction, the number of Fe atoms per unitary formula and the molecular weight of the orthoferrite REFO, respectively. $A_{\propto Fe}$ and A_{REFeO3} are the alpha- iron and the orthoferrite sub-spectral areas, respectively. By assuming that the values for the occupation fractions of the alpha-iron and orthoferrites are equal to one, the Fe atoms by unitary formula of the alpha-iron and the orthoferrites are also equal to one and by introducing the molecular weights of the compounds (see Table 1); thus, four simple formulas were obtained to determine F_{REFO}.

3. Experimental

3.1. Synthesis method

All samples were synthesized by self-combustion method. Aqueous solutions in the adequate stoichiometry for each one of the rare-earth nitrates, plus iron nitrate were prepared. The nitrates used were $La(NO_3)_3{\cdot}6H_2O$ (Rodia), $Pr(NO_3)_3{\cdot}6H_2O$ (Rodia), $Nd(NO_3)_3{\cdot}6H_2O$ (Rodia), $Sm(NO_3)_3{\cdot}6H_2O$ (Rodia), and $Fe(NO_3)_3{\cdot}9H_2O$ (Aldrich). Acting as an ignition promoter, glycine $H_2NCH_2CO_2H$ (Merck) was added at the required amounts to get a molar ratio of $NO_3/NH_2 = 1$, which is a proper concentration to guarantee the total formation of complexes with metal cations while increasing their solubility and preventing selective precipitation. The resulting solutions were slowly evaporated at ~400 K until vitreous gels were obtained. The gels were heated up to approximately 550 K when an auto ignition reaction and rapid combustion took place, producing powdered precursors which might still contain carbon residues. Calcinations at 900 K for 10 h were performed to eliminate all the remaining carbon (if there was any) and promote the crystallinity.

3.2. Characterization

Structural properties and phase control were analyzed through X-ray diffraction patterns, which were taken using a Panalytical ÝPERT PRO MPD diffractometer with $CuK_{\alpha 1}$ radiation (1.5406 Å), operated at 45 kV and 40 mA. The diffraction patterns were recorded at intervals (2θ) from 10° to 90° with a scanning step size of 0.013° during 59 s per step. Rietveld refinement was done by using FullProf software with 22 parameters refined.

Table 1
Molecular weights and C_{REFO} values from Eq. (6) for α-iron and rare-earth orthoferrites REFO ($LaFeO_3$ = LFO, $PrFeO_3$ = PFO, $NdFeO_3$ = NFO, $SmFeO_3$ = SFO).

Compound	α-Fe	LFO	PFO	NFO	SFO
MW_n [g/mol]	55.9	242.8	244.8	248.1	254.2
C_{REFO}	1	4.35	4.38	4.44	4.55

A Scanning Electron Microscopy Philips CM120 instrument operated at an acceleration voltage of 20 kV was used to study the morphology and to perform the microanalysis of the samples.

Absorbers for Mössbauer spectroscopy in transmission mode were prepared for each sample. Measurements were done with a 100 mCi ^{57}Co source in a Rh matrix, which was driven at a constant acceleration rate in a triangular mode at room temperature. The spectra were recorded in 512 channels and the Lorentzian lines of the folded data were fitted using the Recoil software [20]. The spectrometer was calibrated with the room temperature spectrum of an α-Fe foil. All isomer shift values were expressed relative to the centroid of this spectrum.

3.3. Preparation of samples for F-factor calculations

In order to calculate F_{REFO} relative to α-Fe, absorbers were prepared as a homogenous mixture of the orthoferrite sample, and the reference material α-Fe. Sugar was added to fill the entire sample holder. To estimate an error the procedure was repeated three times for different amounts of the compounds as reported in Table 2. Considering that the orthoferrite compound present a high thermal stability, all the procedures were performed at RT no reaction could take place between $REFeO_3$ and ⟨alpha⟩-iron.

With the purpose of choosing the appropriate amount of sample to prepare the absorber, the ideal thickness (t_{ideal}), which is defined as the absorber thickness that gives the largest signal to noise ratio for a given measurement time, was calculated for each one of the samples and for the reference material by using the following equation [21]:

$$t_{ideal} = \frac{1}{\sum_i m_i \mu_{e,i}}, \tag{7}$$

where m_i represents the mass fraction of the i-element in the absorber and $\mu_{e,i}$ is the electronic mass absorption coefficient for the 14.4 keV Mössbauer γ-rays of the i-element. In this way, the calculated t_{ideal} for α-Fe was found to be 15.625 mg/cm^2 and considering the holder diameter, its ideal mass was 19.79 mg. The respective values for the orthoferrite compounds are shown in Table 2.

Another concept taken into account at this point was the thin absorber thickness, t_{thin}, defined as the largest thickness for which their effects are negligible [16]. The dimensionless version of this condition is $t_{a,thin} \ll 1$ and is given by:

$$t_{a,i} = f_i n_i \sigma_0 = \frac{f_i N_i \sigma_0}{A} \tag{8}$$

where σ_0 (2.4×10^{-10} cm^{-1}) is the cross section at resonance for the Mössbauer transition and n_i is the total number of ^{57}Fe atoms of the compound in the area of the holder. Now considering Eq. (4), this can be written as:

$$t_{a,i} = \frac{f_i N_0 m_i a O_i N_{i,m} \sigma_0}{M W_i A} \tag{9}$$

According to Eq. (9), in order to calculate the dimensionless thickness it is necessary to know the *fi*-factor value. We performed the thickness correction of the spectra as it is implemented in the Recoil software (for details see reference [21–23]). The dimensionless thickness for the absorbers was calculated with the results for the f-factors found by using the thickness corrected spectra (See Table 2). As it can be noticed, all the masses that were considered to perform the measurements were under their respective ideal masses values ($m_{REFO} < m_{REFO,ideal}$ and $m_{\alpha\text{-}Fe} < m_{\alpha\text{-}Fe,ideal}$).

Table 2
Orthoferrites and α-Fe masses used to prepare the different absorbers. The corresponding ideal absorber mass and thickness (Eq. (7)) are also displayed.

Sample	Absorbent	m_{REFO} [mg]	$m_{\alpha\text{-}Fe}$ [mg]	t_{ideal} [mg/cm^2]	$m_{REFO\ ideal}$ [mg]
LFO	M1	10.8	9.9	17.0	21.6
	M2	6.5	5.9		
	M3	2.1	2.0		
PFO	M1	10.1	9.7	16.2	20.5
	M2	6.1	5.8		
	M3	2.2	2.1		
NFO	M1	9.6	9.9	15.1	19.2
	M2	5.7	6.0		
	M3	1.9	2.0		
SFO	M1	9.5	9.8	14.0	17.8
	M2	5.6	5.9		
	M3	2.0	2.1		

4. Results and discussion

4.1. X-ray diffraction analysis and rietveld refinement

The crystal structure and phase purity of the rare-earth orthoferrites $REFeO_3$ (RE = rare-earth La, Pr, Nd and Sm) were studied by X-ray diffraction (XRD). The XRD patterns of the samples after calcination show a well-defined characteristic peak for this structure at ~32° which is in good agreement with JCPDF cards [22,23] (see Fig. 1). Segregated phases were not observed, indicating that the synthesis method produced single phase compounds.

The structure of the REFO phases was determined by Rietveld refinement of XRD data. The four compounds were fitted into the space group *Pbnm* with an orthorhombic symmetry, where the iron atoms are octahedrally coordinated (FeO_6) and the rare-earth (RE) atoms are located in the interstices (see Fig. 1(c) as an example). In this structure, the atomic position of the rare-earth atom was displaced from the ideal cubic position, generating the octahedral tilted around the b and c orthorhombic axes. This phenomenon was most evident in the Fe—O—Fe bond angles that were lower than the ideal value of 180° [25]. To a large extent, the degree of tilting was determined by the size of the RE ions; the larger the Re ion, the smaller the tilting and the Fe—O—Fe bond angle as it approaches to 180° [12]. This is clear in Table 3, in which the refined structural parameters, selected bond lengths and bond angles are summarized. As can be seen, the cell volume increases with the cell parameter *c* associated with the elongation of the ideal cubic cell, while the Fe—O—Fe angle decreases with the RE ion radii as expected. This smaller change in the bond parameters will affect the superexchange interactions and thus, the Neel temperature (T_N). Effectively, a variation in the calculated T_N of REFO orthoferrites was observed. T_N variation with Fe—O—Fe bond angles data (θ_1 = Fe—O_1—Fe and θ_2 = Fe—O_2—Fe) reported in Table 3 is given by the relation [26]: $T_N = -1/3 \times T_0 \times [\cos(\theta_1) + 2 \times \cos(\theta_2)]$, where T_0 is the value (770 K) of the Neel point of an hypothetical orthoferrite with linkage angles of 180°. The calculated T_N of LFO, PFO, NFO and SFO were 718, 697, 684 and 673 K, respectively. This result is in good agreement with that reported in orthoferrites by Traves et al. [26]. However, the calculated T_N of REFO are different between them, due to the possible changes in the spacing between the magnetic Fe^{3+} ions (the average size of RE ions increases). Additionally, the average crystal sizes (D) were estimated from the X-ray line broadening using the Scherrer's equation: $D = 0.89\lambda/\beta\cos(\Theta)$, where λ is the wavelength of the X-ray radiation (0.154056 nm), β is the full width at half maximum (FWHM) and θ is the diffraction angle. In this way, the average crystallite size was estimated to lie between 55 and 76 nm for the four compounds.

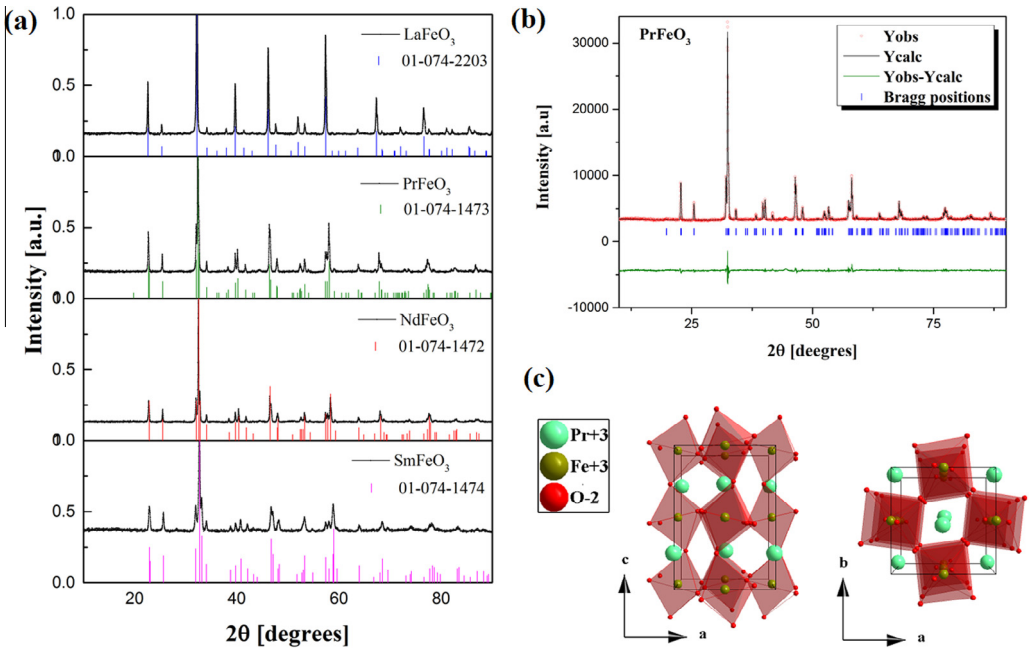

Fig. 1. (a) X-ray diffraction patterns of orthoferrites RE FeO_3 (RE = rare-earth La, Pr, Nd and Sm). (b) Rietveld refinement for the X-ray diffractogram of $PrFeO_3$ using Fullprof [24]. (c) Orthorhombic distorted structure of $PrFeO_3$.

Table 3
Refined structural parameters of $REFeO_3$ (RE = rare-earth La, Pr, Nd and Sm) phases obtained from self-combustion method. Crystal system = Orthorhombic, Space group = Pbnm (N° 62).

Compound	LFO	PFO	NFO	SMO
Lattice parameters [Å]	a = 5.55050(6)	a = 5.48390(6)	a = 5.45361(6)	a = 5.40297(6)
	b = 5.56212(7)	b = 5.57395(7)	b = 5.58538(7)	b = 5.59128(7)
	c = 7.86486(8)	c = 7.78816(8)	c = 7.76401(8)	c = 7.71339(8)
Cell volume [$Å^3$]	242.8	238.1	236.5	233.0
*Re (x, y, 0.25) (**4c**)*				
X	0.0039(13)	0.99052(13)	0.98843(13)	0.98803(13)
Y	0.0287(14)	0.04282(14)	0.04789(14)	0.05437(14)
*Fe (0, 0.5, 0) (**4b**)*				
*O_1 (x, y, 0.25) (**4c**)*				
X	0.072(15)	0.08313(15)	0.08900(15)	0.09844(15)
Y	0.492(16)	0.48680(16)	0.48247(16)	0.46299(16)
*O_2 (x, y, z) (**8d**)*				
X	−0.28090(17)	0.72204(17)	0.70736(17)	0.71561(17)
Y	0.28150(18)	0.28603(18)	0.29133(18)	0.29103(18)
Z	0.03940(19)	0.04361(19)	0.04262(19)	0.04680(19)
R factors [%]				
R_p	22.29	23.17	22.91	27.84
R_{wp}	13.52	12.58	12.91	14.03
R_{exp}	7.61	8.97	8.27	12.00
χ^2	3.16	1.96	2.44	1.37
Bond lengths [Å]				
Fe–O_1 × 2	1.9941	2.0010	2.0032	2.0110
Fe–O_2 × 2	1.9556	1.9650	2.0037	1.9638
Fe–O_2' × 2	2.0474	2.0347	2.0090	2.0335
Bond angles [°]				
Fe–O_1–Fe	160.8	153.3	151.4	147.0
Fe–O_2–Fe	157.9	155.6	153.2	153.1
Average crystal size [nm]	55.3	72.1	75.3	69.9

4.2. Surface morphology and elemental compositions

Scanning electron micrographs for RE FeO_3 perovskites are depicted in Fig. 2. The images show systems that have micro and macro porosities with open flakes type morphologies, associated with the synthesis method, where the gel precursors were exposed to high temperatures and gas flow in short period of time. In this morphology, occasionally gases, such as CO_2, in the environment were trapped due to the base nature of the lanthanides and the BET specific surface area of around 10 m^2/g [27].

Elemental composition of the materials was estimated using EDX and the atomic percentages of RE (La, Pr, Nd, Sm), iron, and oxygen are listed in Table 4. In this table, it can be observed that RE/Fe ratio was almost equal to unity for all perovskites, indicating the incorporation of the elements on the structure and confirming the absence of residual oxides.

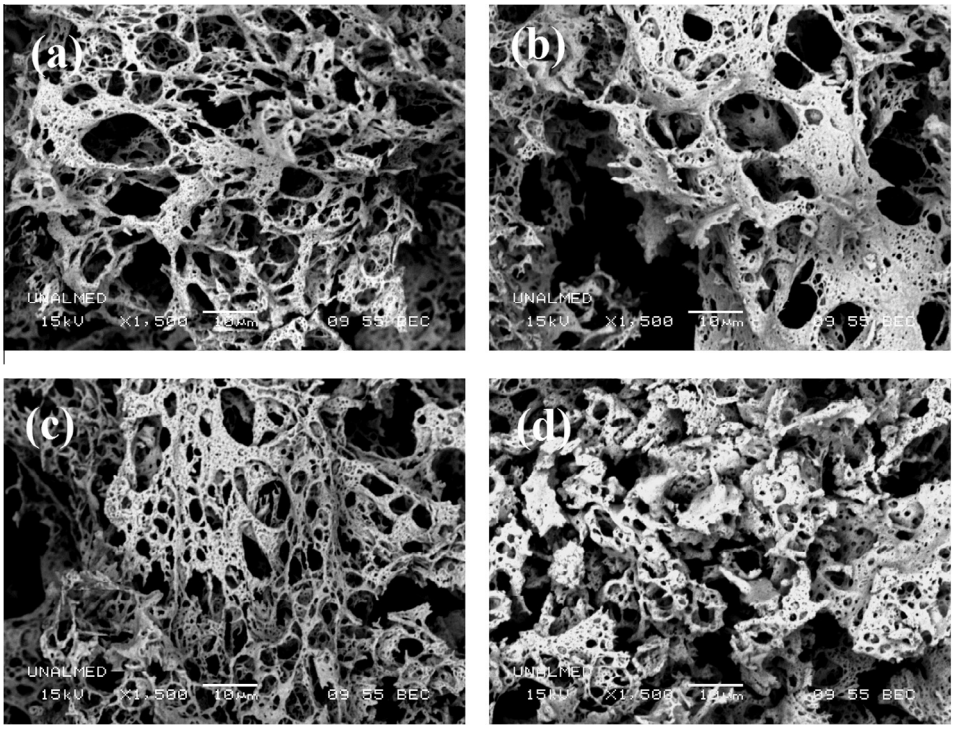

Fig. 2. SEM micrographs of orthoferrites phases obtained from self-combustion method. (a) $LaFeO_3$, (b) $PrFeO_3$, (c) $NdFeO_3$ and (d) $SmFeO_3$.

Table 4
Elemental composition of $REFeO_3$ (RE = rare-earth La, Pr, Nd and Sm) phases estimated from EDX.

Sample	Nominal atomic composition			RE/Fe
	RE	Fe	O	
LFO	21.53	22.48	55.99	0.96
PFO	22.85	23.00	54.15	0.99
NFO	22.33	23.69	53.98	0.94
SFO	22.21	23.17	54.62	0.96

Table 5
Hyperfine parameters of $REFeO_3$ orthoferrites and α-Fe before mix, derived from the fitting of their RT Mössbauer spectra. Estimated errors are in the order of ±0.01 mm/s for isomer shift (δ), quadrupole shift (ε), and line width (Γ) and about ±0.1 T for the magnetic hyperfine field (B).

Site parameters	LFO	PFO	NFO	SFO	α-Fe
δ [mm/s]	0.37	0.36	0.36	0.36	0.00
ε [mm/s]	−0.03	−0.01	−0.01	−0.05	0.00
B [T]	52.2	51.3	51.1	50.1	33.0
Γ [mm/s]	0.15	0.19	0.20	0.21	0.17
χ^2	0.74	1.80	1.62	1.18	1.45

The above results, confirm the assumption that occupation fraction of the alpha iron and orthoferrites are equal to one. This assumption is supported reasonably well by the elemental composition of REFO phases estimated from EDX analysis (see Table 4) and by the Rietveld refinement results, in which the absence of other phases was confirmed and the occupation fraction was calculated getting close to 1 (see Table 3).

4.3. Mössbauer spectroscopy and relative recoilless fraction (F) determination

Mössbauer spectroscopy at room temperature was used as structural and magnetic complementary characterization technique. All spectra were fitted by introducing a sextet with values of isomer and quadrupole shift, which are in good agreement with the crystallographic structure and the stoichiometry of the compound (Table 5). In the orthoferrites, the iron atoms are in

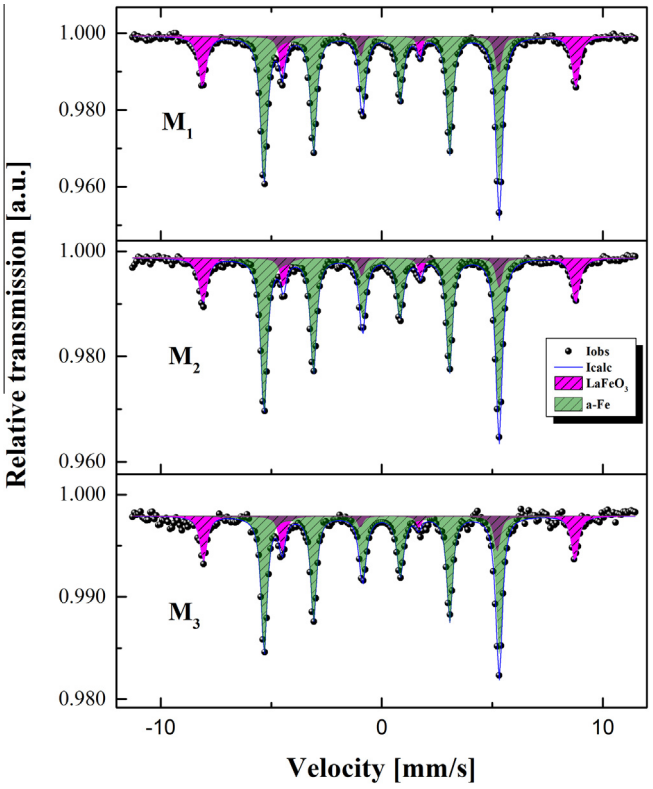

Fig. 3. Typical thickness-corrected RT Mössbauer spectra for the three absorbers M1, M2 and M3 obtained from different mixtures of $LaFeO_3$ with α-Fe as reported in Table 2.

equivalent sites with a $3d^5$ configuration, in an octahedral coordination and with an oxidation state of Fe^{+3}.

As mentioned above, the Mössbauer spectra for REFO were fitted with a sextet (see Fig. 3 where the sextet with the most intense line corresponds to α-Fe and the other one to $LaFeO_3$ phase). The high magnetic fields involved imply that these kinds of compounds have a magnetic behavior at room temperature. While the orthoferrites have an antiferromagnetic behavior at RT associated to a super-exchange interaction between iron ions Fe^{3+}–Fe^{3+}; a spin canting phenomenon produced by a DM interaction has been shown to cause a weak ferromagnetism, which makes the obtained results feasible [4,25]. It is interesting to note, that there is a good correlation between the intensity of the magnetic hyperfine field (see Table 5) on the one hand, and the cell volumes. Similarly, there is a good correlation among Fe—O_1 bond lengths and Fe—O_1—Fe bond angles (see Table 3). From Table 5, it is clear that, within experimental error, *B* decreases for the samples in the following order: $LaFeO_3$ > $PrFeO_3$ > $NdFeO_3$ > $SmFeO_3$. Similarly, from Table 3, it is seen that both cell volumes and Fe—O_1—Fe bond angles also decrease in the same order. On the contrary, Fe—O_1 bond lengths increases following the same pattern as previously mentioned (see Fig. 4). These results mean that the super-exchange interactions between the Fe ions, mediated by the oxygen ions, are directly affected by the bond lengths and bond angles, which in turn affect the magnitude of the hyperfine field.

The areas of each one of the thickness-corrected sextets are summarized in Table 6 and were used to calculate F_{REFO} (Table 7).

Finally by using Eq. (3) and the reported absolute (*f*) factor value of 0.7 for α-Fe [28,29], the absolute recoilless (*f*) factors for the orthoferrite compounds were calculated (Table 8).

The absolute *f*-factor values were also calculated by using the Debye model of thermal motion of atoms and the Debye temperatures reported for these compounds [12] and by using the Recoil Software. The results of this analysis are presented in Table 9.

The relative recoilless F fractions for the rare-earth orthoferrites with respect to α-Fe are greater than one, which implies that the probability to find recoilless events in the REFO compounds is greater than in α-Fe. These results could be attributed in a large extent to the crystal Debye temperature of the REFO compounds which is greater than the α-Fe one (Θ_D (α-Fe) is 345 K). This means that the orthoferrites are more thermally stable. In turn, this implies that the iron nucleus is strongly embedded avoiding the recoilless phenomenon and therefore is easier to show the absorption of γ-rays at room temperature. This thermal stability may be

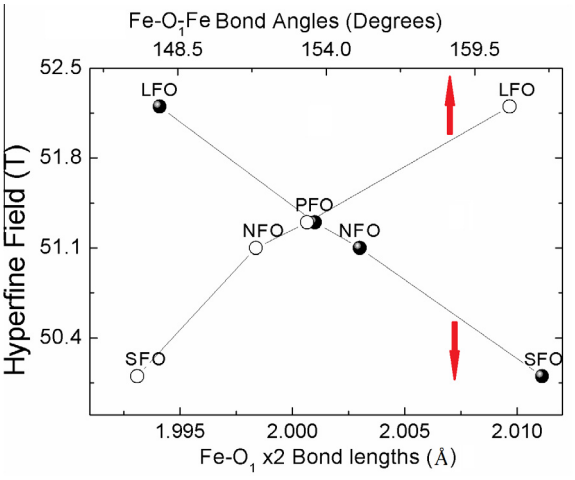

Fig. 4. Hyperfine field, B(T) as a function of Fe—O_1 × 2 bond lengths (arrow down) and Fe—O—Fe bond angles (arrow up).

Table 6
Sub-spectral areas for the thickness-corrected room temperature Mössbauer spectra corresponding to the three different absorbers obtained from mixtures for each one of the orthoferrite compounds and α-Fe, as reported in Table 2.

Compound	Absorber	After thickness correction [%]	
		REFO area	α-Fe area
LFO	M1	25.1	74.9
	M2	24.6	75.4
	M3	24.3	75.7
PFO	M1	19.7	80.3
	M2	20.8	79.2
	M3	20.8	79.2
NFO	M1	20.8	79.2
	M2	21.1	78.9
	M3	19.3	80.7
SFO	M1	19.1	80.9
	M2	18.1	81.9
	M3	24.1	75.9

Table 7
Relative recoilless F fractions for the three different absorbers obtained from mixtures of the orthoferrites and α-Fe and average values $\bar{x}$.

Sample	F_{LFO}	F_{PFO}	F_{NFO}	F_{SFO}
M1	1.335	1.037	1.187	1.094
M2	1.287	1.094	1.234	1.046
M3	1.329	1.098	1.103	1.180
$\bar{x}$	1.31 ± 0.02	1.07 ± 0.04	1.17 ± 0.07	1.11 ± 0.07

Table 8
Average recoilless (*f*) factors for $REFeO_3$ (RE = rare-earth La, Pr, Nd and Sm) calculated using Eq. (3).

Sample	f_{LFO}	f_{PFO}	f_{NFO}	f_{SFO}
$\bar{x}$	0.92 ± 0.02	0.75 ± 0.04	0.82 ± 0.07	0.78 ± 0.07

Table 9
Room temperature recoilless (*f*) factors for $REFeO_3$ (RE = rare-earth La, Pr, Nd and Sm) calculated using the Debye model and the Debye temperatures reported by Eibschütz et al. [12].

$REFeO_3$	Θ_D [K]	*f* Debye model
LFO	800 ± 50	0.927
PFO	780 ± 50	0.924
NFO	770 ± 50	0.922
SFO	730 ± 50	0.915

associated with the structure type of the REFO compounds, where as seen before in Section 4.1, the Fe atom is confined into a FeO_6 octahedral site and linked by ionic bounds while in α-Fe the atoms are linked by metallic bounds with dense planes where heat is easily conducted.

The above results shown a discrepancy in the absolute *f*-factors reported in Tables 8 and 9, with an average relative error around 11% in comparison with the values predicted by the Debye model. This discrepancy can be explained by several reasons. The Debye theory is a too ideal approximation for modeling the complex lattice vibrations of iron ions in orthoferrites. The Debye model applies to isotropic materials in a crystalline phase and perhaps, this is not the case for the orthoferrites in this work. Moreover, the large uncertainties in the Θ_D values can affect the calculated absolute *f*-factors. On the other hand, it is also probable that the absolute *f*-factor of the powder α-Fe that we have used (0.7) be somehow different from the real value of our sample. In fact this value is very sensitive to particle grain size and chemical and physical properties of the compound.

5. Conclusions

The $REFeO_3$ compounds with RE = rare-earth, La, Pr, Nd, and Sm were successfully synthesized by self-combustion method. From XRD and Mössbauer spectroscopy analysis, a direct correlation between the magnitude of the magnetic hyperfine field (B) on the one hand and Fe—O_1—Fe bond angles on the other hand was found. On the contrary, an indirect relation between B and the Fe—O_1 bond length was observed. By using bond angles data of REFO orthoferrites and assuming a dependence of superexchange interaction on Fe—O—Fe linkage angle, the Neel temperatures were calculated with values ranging between 718 and 673 K. The recoilless F factors of each orthoferrites were experimentally determined relative to α-Fe at room temperature with values equal to 1.30 ± 0.02, 1.08 ± 0.04, 1.15 ± 0.05, and 1.18 ± 0.08 for $REFeO_3$, with RE = rare-earth, La, Pr, Nd, and Sm, respectively. All values were greater than 1, suggesting that iron ions are located in a more rigid lattice in the orthoferrites than in α-Fe.

References

[1] R.L. White, J. Appl. Phys. 40 (1969) 1061.
[2] R. White, R. Nemanich, C. Herring, Phys. Rev. B 25 (1982) 1822–1836.
[3] T. Moriya, Phys. Rev. 120 (1960) 91–98.
[4] W. Slawinski, R. Przenioslo, I. Sosnowska, E. Suard, J. Phys.: Condens. Matter 17 (2005) 4605–4614.
[5] R. Przeniosło, I. Sosnowska, P. Fischer, W. Marti, F. Bartolomé, J. Bartolomé, E. Palacios, R. Sonntag, J. Magn. Magn. Mater. 160 (1996) 370–371.
[6] A. Maziewski, R. Szymczak, J. Phys. D Appl. Phys. 10 (1977) L37.
[7] W. Zhao, S. Cao, R. Huang, Y. Cao, K. Xu, B. Kang, J. Zhang, W. Ren, Phys. Rev. B 91 (2015) 104425.
[8] H. Wu, S. Cao, M. Liu, Y. Cao, B. Kang, J. Zhang, W. Ren, Phys. Rev. B 90 (2014) 144415.
[9] S. Cao, H. Zhao, B. Kang, J. Zhang, W. Ren, Sci. Rep. 4 (2014) 5960.
[10] P. Emsbo, P.I. McLaughlin, G.N. Breit, E.A. du Bray, A.E. Koenig, Gondwana Res. 27 (2015) 776–785.
[11] K. Binnemans, P.T. Jones, B. Blanpain, T. Van Gerven, Y. Yang, A. Walton, M. Buchert, J. Cleaner Prod. 51 (2013) 1–22.
[12] M. Eibschütz, S. Shtrikman, D. Treves, Phys. Rev. 156 (1967) 562–577.
[13] E. Murad, Phys. Chem. Miner. (1996) 248–262.
[14] D.P.E. Dickson, F.J. Berry, Mössbauer Spectroscopy, University Press, 2005.
[15] S.J. Oh, D.C. Cook, J. Appl. Phys. 85 (1999) 329–332.
[16] D.G. Rancourt, Nucl. Instrum. Methods Phys. Res. Sect. B 44 (1989) 199–210.
[17] C. Barrero, K.E. García, J. Chem. Phys. 139 (2013) 034703.
[18] A. Vértes, I. Czakó-Nagy, Electrochim. Acta 34 (1989) 721–758.
[19] E. De Grave, A. Van Alboom, Phys. Chem. Miner. (1991) 337–342.
[20] K. Lagarec, D.G. Rancourt, Recoil-Mössbauer Spectral Analysis Software for Windows, Version 1.02, University of Ottawa, Ottawa, 1998.
[21] G. Long, T. Cranshaw, G. Longworth, Mössbauer Eff. Ref. Data 6 (1983) 42–49.
[22] M. Marezio, J. Remeika, P. Dernier, Acta Crystallogr. Sect. (1970).
[23] M. Marezio, P.D. Dernier, Mater. Res. Bull. 6 (1971) 23–29.
[24] J. Rodrigues-Carvajal, FULLPROF: a program for Rietveld refinement and pattern matching analysis, Lab. Leon Brillouin, CEA-CNRS, Fr., 2000.
[25] S.C. Parida, S.K. Rakshit, Z. Singh, J. Solid State Chem. 181 (2008) 101–121.
[26] D. Treves, M. Eibschütz, P. Coppens, Phys. Lett. 18 (1965) 216–217.
[27] S. Farhadi, Z. Momeni, M. Taherimehr, J. Alloys Compd. 471 (2009) L5–L8.
[28] M. Sorescu, J. Nanopart. Res. 4 (2005) 221–224.
[29] M. Sorescu, Mater. Lett. 54 (2002) 256–259.